DOI: 10.1002/ejic.200901254

Synthesis, Crystal Structures, and Magnetic Properties of Mn^{II}, Co^{II}, and Zn^{II} Coordination Polymers Containing 1,2,4,5-Benzenetetracarboxylic Acid and 4,4′-Azobispyridine

Li-Min Zhao,[a] Huan-Huan Li,[a] Ying Wu,[a] Shi-Yuan Zhang,[a] Zhen-Jie Zhang,[a] Wei Shi,[a] Peng Cheng,*[a] Dai-Zheng Liao,[a] and Shi-Ping Yan[a]

Keywords: Solid-state structures / Magnetic properties / Cyclic voltammetry / Coordination polymers / Mixed ligands

Manganese(II), cobalt(II), and zinc(II) coordination polymers, $\{[Mn(H_2btec)(azopy)(H_2O)_2]\cdot(azopy)\}_n$ (**1**), $\{[Co(H_2btec)(azopy)(H_2O)_2]\cdot(azopy)\}_n$ (**2**), and $\{[Zn_{2.5}(btec)(azopy)(\mu_3\text{-}OH)(H_2O)]\cdot H_2O\}_n$ (**3**) (H_4btec = 1,2,4,5-benzenetetracarboxylic acid; azopy = 4,4′-azobispyridine), were synthesized by a hydrothermal method and characterized by single-crystal X-ray diffraction, elemental analysis, and powder X-ray diffraction. Compounds **1** and **2** are isomorphic and crystallize in the triclinic space group $P\bar{1}$, exhibiting a 2D grid framework bridged by two types of ligands. Compound **3** also crystallizes in the triclinic space group $P\bar{1}$ and possess an interesting 3D coordination framework with an unprecedented dodecadentate coordination mode and a unique $\{4^{16}.5^{10}.6^{18}.7\}\{4^4.5.6\}^2$ topological structure. The ideal topology of **3** has not been encountered in metal–organic framework chemistry, which has been deposited in the Reticular Chemistry Structure Resource under the name zim net. Magnetic studies show that there are antiferromagnetic interactions in both **1** and **2**. The cyclic voltammograms of **1**–**3** in the solid state were also obtained.

Introduction

During the past decade, the design and synthesis of crystalline material constructed from molecular clusters linked by extended groups have attracted great attention. Most notable fields are metal–organic frameworks (MOFs),[1–7] in which polyatomic inorganic metal-containing clusters are connected by polytopic linkers. The direct driving forces originate not only from their fascinating topological structures but also from their versatile applications in gas adsorption and separation, catalytic activities, optoelectronic material, luminescence, magnetism, and so on.[8–19] Thus, structural design or modification of the coordination polymers has become a very active field in crystal engineering.[20–24] In this process, judicious selection of ligands as basic building blocks is of great importance because slight structural changes in the organic building blocks such as length, flexibility, and symmetry can dramatically change the structural motifs of coordination polymers. It is well known that organic ligands play a rather important role in the construction of MOFs, and multicarboxylate ligands are frequently chosen owing to their rich coordination modes, coordinating to metal ions through complete or partial deprotonation of their carboxy groups, and their metal binding ability.[25–30]

1,2,4,5-Benzenetetracarboxylic acid (H_4btec) has been well known to be an ideal ligand to encapsulated metal nodes, forming coordination compounds with unique structures and interesting properties,[31–35] which may have the following advantages: (i) Higher symmetry of the ligand may cause the generation of regular structures. (ii) The rigidity of the ligand may reduce the possibility of lattice interpenetration in the products.[36] (iii) The multidentate carboxylate is known to be essential in chelating metal ions to form chain-like units with M–O–M connectivity. (iv) The four carboxylic groups of this ligand may chelate to metal ions by using various coordination modes to form fascinating multidimensional compounds.

In consideration of the varieties of topologies and properties, incorporating functional moieties into MOFs is often a popular method used in crystal engineering. Our approach towards the design and synthesis of new coordination polymers focuses on using aromatic carboxylate ligands like H_4btec in conjunction with secondary co-ligands, such as 4,4′-azobispyridine (azopy).[37–39] As part of our ongoing efforts in the design and synthesis of multifunctional crystalline materials, we report herein three new transition-metal polymers: $\{[Mn(H_2btec)(azopy)(H_2O)_2]\cdot(azopy)\}_n$ (**1**), $\{[Co(H_2btec)(azopy)(H_2O)_2]\cdot(azopy)\}_n$ (**2**), and $\{[Zn_{2.5}(btec)(azopy)(\mu_3\text{-}OH)(H_2O)]\cdot H_2O\}_n$ (**3**).

[a] Department of Chemistry, Nankai University, Tianjin 300071, China
E-mail: pcheng@nankai.edu.cn

Supporting information for this article is available on the WWW under http://dx.doi.org/10.1002/ejic.200901254.

 © 2010 Wiley-VCH Verlag GmbH & Co. KGaA, Weinheim

Results and Discussion

Synthesis

The isolation of compounds **1**, **2**, and **3** depends on the hydrothermal techniques, because differential solubility of organic and inorganic precursors can be minimized. In addition, we know that many factors such as temperature, pH value, metal–ligand stoichiometry, and reaction time can influence the products. Parallel experiments show that the use of LiOH and the appropriate temperature are crucial. LiOH is the key for the formation of these complexes, because it serves to deprotonate the H_4btec ligand and to promote the formation of the bridges from H_2O molecules introduced by the solvent H_2O or the starting metal salts. When no base is added, only clear solutions were obtained, and when using NaOH or KOH to replace the LiOH, impure precipitates were observed. As a result of this process, suitable crystals of **1**–**3** for X-ray diffraction studies were obtained.

Structures of 1 and 2

Single-crystal X-ray diffraction analysis was performed on compounds **1**–**3**, which showed that compounds **1** and **2** are isostructural and crystallize in the triclinic $P\bar{1}$ space group. The structure of **2** is representatively described in detail here. In an asymmetrical unit of **2**, the central Co^{II} ion displays one type of six-coordinate mode (Figure 1) and lies in a distorted octahedral coordination environment completed by two carboxylic oxygen atoms from two independent btec ligands [Co1–O1 2.078(3) Å], two pyridine nitrogen atoms from two azopy molecules [Co1–N1 2.172(3) Å] in the equatorial positions, as well as two terminal water molecules [Co1–O3 2.136(3) Å] in the axial positions. A free azopy molecule exists in the lattice. The Co–N bond length is obviously longer than the Co–O bond length. The *trans* O1–Co–O1A, N1–Co–N1A, and O3–Co–O3A bond angles are crystallographically 180°. On the other hand, the *cis* O–Co–O and O–Co–N bond angles range from 89.45(12) to 91.58(12)°, which is indicative of a very slightly distorted octahedral environment. Additional bond lengths and angles for **1** and **2** are presented in Table 1.

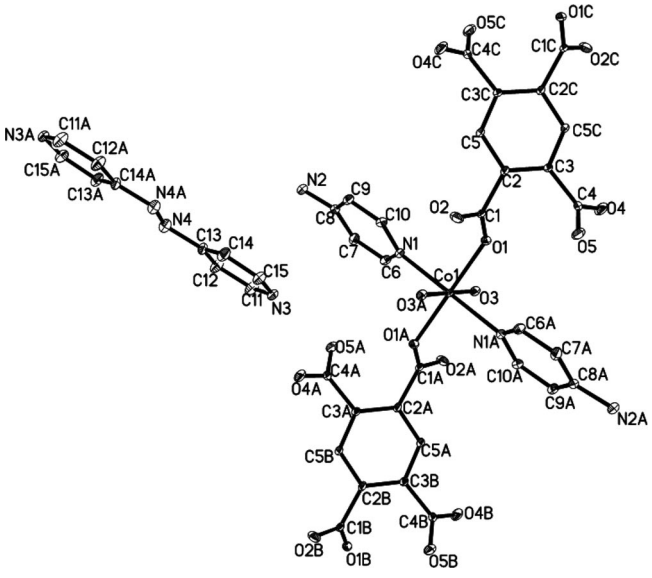

Figure 1. The coordination environment of the Co^{II} ion in **2**. All H atoms are omitted for clarity.

Table 1. Selected bonds lengths/Å and angles/° for compounds **1**–**3**.[a]

	1		
Mn1–O3A	2.147(2)	O3A–Mn1–O3	180.00(12)
Mn1–O3	2.147(2)	O3A–Mn1–O5A	87.35(10)
Mn1–O5A	2.196(3)	O3–Mn1–O5A	92.65(10)
Mn1–O5	2.196(3)	O3A–Mn1–O5	92.65(10)
Mn1–N3	2.280(3)	O3–Mn1–O5	87.35(10)
Mn1–N3A	2.280(3)	O5A–Mn1–O5	180.0
O3A–Mn1–N3A	91.69(11)	O3A–Mn1–N3	88.31(11)
O3–Mn1–N3A	88.31(11)	O3–Mn1–N3	91.69(11)
O5A–Mn1–N3A	91.89(11)	O5A–Mn1–N3	88.11(11)
O5–Mn1–N3A	88.11(11)	O5–Mn1–N3	91.89(11)
	2		
Co1–O1	2.078(3)	O1–Co1–O3	90.55(12)
Co1–O1A	2.078(3)	O3A–Co1–O3	180.000(1)
Co1–O3	2.136(3)	O1A–Co1–N1	88.42(12)
Co1–O3A	2.136(3)	O1–Co1–N1	91.58(12)
Co1–N1	2.172(3)	O3A–Co1–N1	91.31(13)
Co1–N1A	2.172(3)	O3–Co1–N1	88.69(14)
		O1A–Co1–N1A	91.58(12)
O1A–Co1–O1	180.00(14)	O1–Co1–N1A	88.42(12)
O1A–Co1–O3A	90.55(12)	O3A–Co1–N1A	88.69(14)
O1–Co1–O3A	89.45(12)	O3–Co1–N1A	91.31(13)
O1A–Co1–O3	89.45(12)	N1–Co1–N1A	180.000(1)
	3		
Zn1–O10A	2.053(4)	O10A–Zn1–O10A	180.0(3)
Zn1–O10B	2.053(4)	O10A–Zn1–O3	89.27(18)
Zn1–O3	2.075(5)	O10B–Zn1–O3	90.73(18)
Zn1–O3A	2.075(5)	O10A–Zn1–O3B	90.73(18)
Zn1–O5	2.156(4)	O10B–Zn1–O3C	89.27(18)
Zn1–O5A	2.156(4)	O3–Zn1–O3C	180.00(6)
Zn2–O4A	2.042(5)	O4A–Zn2–O1	98.8(2)
Zn2–O1	2.067(5)	O4A–Zn2–O8A	168.7(2)
Zn2–O8A	2.082(5)	O1–Zn2–O8A	89.30(19)
Zn2–O10	2.098(4)	O1–Zn2–O10	91.19(19)
Zn2–O5A	2.155(5)	O10–Zn3–O6A	97.7(2)
Zn3–O10	1.982(5)	O2–Zn3–O6A	159.7(2)
Zn3–O9	2.027(6)	O10–Zn3–O8	98.40(19)

[a] For compound **1**, A: $-x + 1, -y, -z + 1$; for compound **2**, A: $-x + 1, -y + 1, -z + 1$; for compound **3**, A: $-x + 1, -y + 2, -z$; B: $x - 1, y, z$; C: $-x, -y + 2, -z$.

In **1** and **2**, one type of 1D chains are composed of btec ligands bridging between two metal ions through a pair of carboxylato groups in one direction (Figure 2). The btec carboxylate groups are not coplanar with their parent benzene ring, and the dihedral angles between the coordinated carboxylato groups and the aromatic ring are quite similar (48.85 and 49.97° for **1** and **2**, respectively), as are the dihedral angles between the uncoordinated carboxylate groups and the aromatic ring: 42.58 and 40.02° for **1** and **2**, respectively. The azopy co-ligand shows direct bridging to the central metal atoms to form Co–azopy–Co chains. The two types of 1D chains intersect each other to form a 2D grid

 © 2010 Wiley-VCH Verlag GmbH & Co. KGaA, Weinheim

structure with window dimensions of 11.25×13.32 Å^2, and the free ligands as guest molecules in a repetitive and spatial arrangement are located in the lattice.

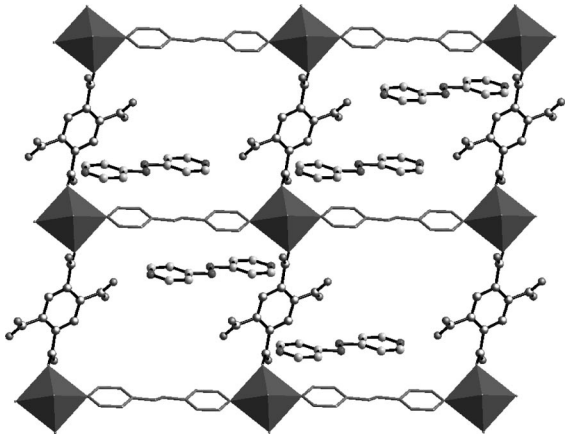

Figure 2. View of the 2D network of **2**. All H atoms are omitted for clarity.

Structure of 3 and Zim Topological Net

Compound **3** possess a 3D framework and crystallizes in a triclinic system in the space group $P\bar{1}$, whose building unit is $[Zn_{2.5}(btec)(azopy)(\mu_3\text{-}OH)(H_2O)]$. In the asymmetric unit, there are three types of coordination environments around the zinc(II) ions (Figure 3). Zn1 has a slightly distorted octahedral configuration, completed by two carboxylic oxygen atoms from two different btec ligands [Zn1–O3 2.075(5) Å], two hydroxy groups [Zn1–O10A 2.053(4) Å] in the equatorial positions, as well as another two carboxylic oxygen atoms from two different btec ligands [Zn1–O5 2.156(4) Å] in the axial positions. The Zn2 and Zn3 atoms are both in a distorted octahedral coordination environment. Zn2 is defined by four carboxylic oxygen atoms from four different btec ligands and one hydroxy group and one pyridine nitrogen atom from the azopy molecule. The Zn2–O distances are in the range 2.042(5)–2.155(5) Å, and the Zn2–N1 distance is 2.173(6) Å. Similarly, the Zn–N bond length is obviously longer than the Zn–O bond length in the crystal structure, which is also due to the different radii of the nitrogen and oxygen atoms. Zn3 is surrounded by four carboxylic oxygen atoms from three different btec ligands with one chelated carboxylic group, one hydroxy group shared with Zn2, as well as one terminal water molecule. The Zn3–O distances are in the range 1.982(5)–2.473(6) Å. Additional bond lengths and angles for **3** are presented in Table 1.

It is worthy to note that the btec ligands are all deprotonated and take two different kinds of coordination environments around it. One has an unprecedented dodecadentate coordination mode, as a $\mu_8\text{-}\eta^3\eta^3\eta^3\eta^3$ linker to connect eight zinc(II) ions, and the dihedral angles between the carboxylic groups and the aromatic ring are 16.15 and 72.90°, respectively. Another has an octadentate bridging mode and also links eight zinc(II) ions, and each carboxylic group adopts

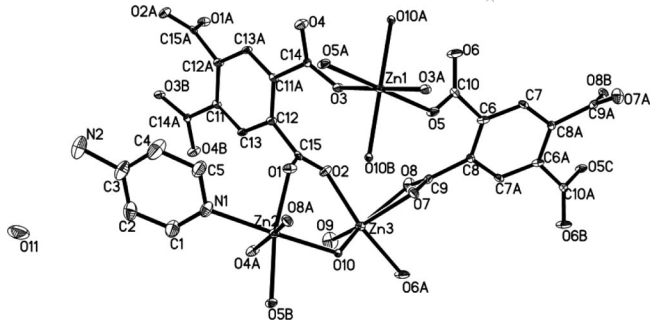

Figure 3. The coordination environment of the Zn^{II} ions in **3**. All H atoms are omitted for clarity.

a $\mu_2\text{-}\eta^1\eta^1$ mode (Figure 4). To the best of our knowledge, this is the first case of dodecadentate coordination; it has not been observed previously.

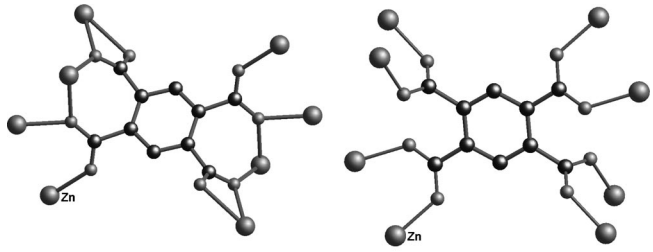

Figure 4. The two coordination modes of the $btec^{4-}$ ligand in **3**: (a) dodecadentate and (b) octadentate.

In the configuration, there is a Zn_5O_2 center dissymmetrical SBU (second-building unit) bridging with two μ_3-OH. The distances between the adjacent Zn^{II} ions are in the range 3.135–3.470 Å (Figure 5). Through different kinds of coordination modes of the carboxylic groups, the SBU was linked to form a 1D $(ZnO)_n$ cluster chain along the *a* axis (Figure 6). It is interesting that the five zinc atoms are coplanar, which results in a clear crystallographic plane when viewed along the *c* direction (grey thin plane in Figure 6).

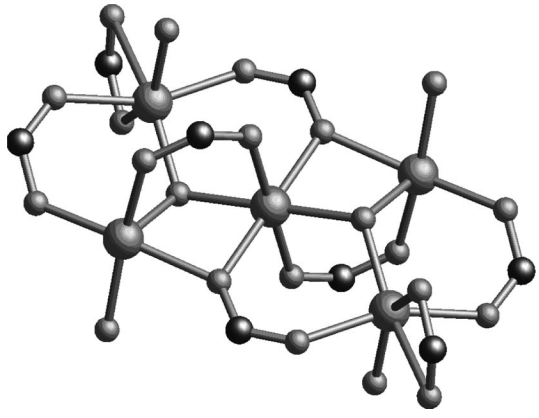

Figure 5. The second-building unit in **3**.

 © 2010 Wiley-VCH Verlag GmbH & Co. KGaA, Weinheim

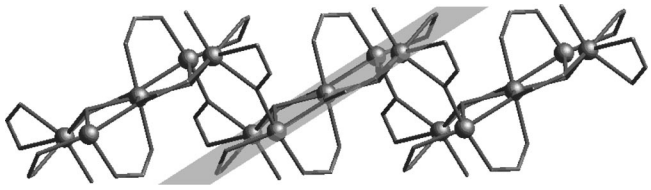

Figure 6. The 1D Zn cluster chain viewed along the *c* direction in compound **3**.

As shown in Figure 7, two coordination modes of the $btec^{4-}$ ligands connect the SBU cluster chain to produce a 3D architecture with rhomboid windows of 17.39×15.02 Å^2, and the central Zn^{II} ions of the SBU are located at the vertexes of the rhombus. Furthermore, the azopy molecules adopt bidentate modes and link the two Zn^{II} ions on the diagonal positions, which may prevent interpenetration of the structural units and enhance the stabilization of the compound.

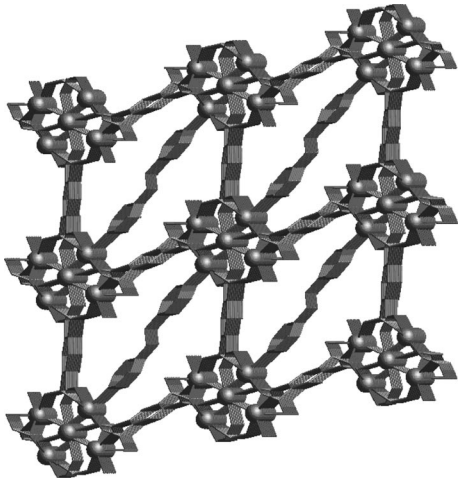

Figure 7. The 3D architecture of compound **3** viewed from the *a* direction.

The 3D network of **3** can be interpreted topologically as a novel (4,4,10)-connected 2-nodal net simplified with topos and systre, and this net has the point (Schlafli) symbol $\{4^{16}.5^{10}.6^{18}.7\}\{4^4.5.6\}^2$ when the Zn clusters act as 10-connected nodes and the two kinds of btec ligands are simplified as topologically equivalent 4-connected nodes (Figure 8). The topology of this net has not appeared in MOF chemistry and has been deposited in the Reticular Chemistry Structure Resource (RSCR) under the name zim net.[40]

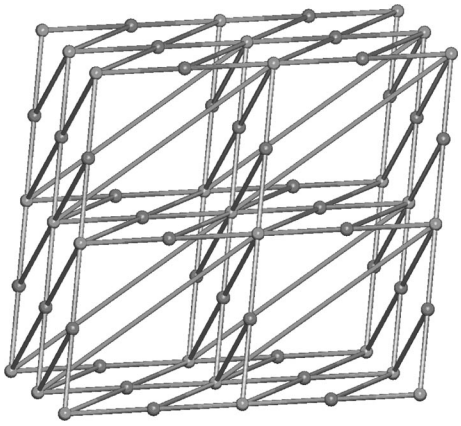

Figure 8. The structural topology of **3**.

PXRD

In order to confirm the phase purity of the bulk materials, the powder X-ray diffraction (PXRD) patterns have been carried out for **1**–**3** at room temperature. The peak positions of the simulated and experimental PXRD patterns are in agreement with each other (Figure S1, Supporting Information), demonstrating the good phase purity of the compounds.

Magnetic Properties of 1 an

The variable-temperature (2–300 K) magnetic susceptibilities of compounds **1** and **2** were measured on crystalline samples in a field of 1 KOe. The temperature dependence of χ_M and $\chi_M T$ for compound **1** is shown in Figure 9. Upon cooling from 300 K, there is a slightly decrease in the value of $\chi_M T$ close to 4.37 emu K mol^{-1} at 300 K to 4.31 emu K mol^{-1} at 50 K. With a further decrease in temperature, the value of the $\chi_M T$ product decreases sharply, reaching a minimum value of 3.95 emu K mol^{-1} at 2 K. The molar magnetic susceptibility per Mn^{2+} ion obeys the Curie–Weiss law [$\chi = C/(T - \theta)$] very well with a Weiss constant $\theta = -0.68$ K and a Curie constant $C = 4.38$ cm^3 mol^{-1} K (Figure S2, Supporting Information). The Curie constant corresponds to one spin-only Mn^{II} ion with $S = 5/2$. The decrease in $\chi_M T$ and the negative Weiss constant suggest antiferromagnetic interactions.

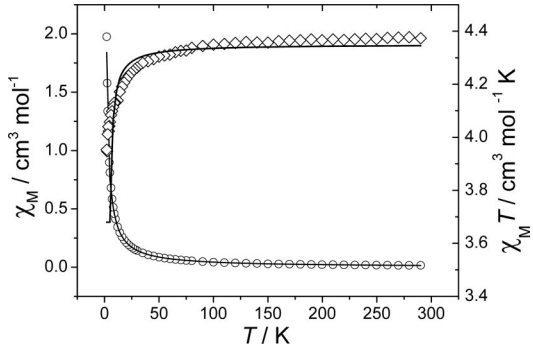

Figure 9. Plot of χ_M (diamond) and $\chi_M T$ (circle) of **1** and the corresponding fit according to the equation.

For an infinite 2D square lattice composed of classical spins ($S = 5/2$) isotropically coupled, the theoretical magnetic susceptibilities is given by Equation (1).[41]

$$\chi = \frac{\left[Ng^2\beta^2 S(S+1)(1+u)^2\right]}{\left[3kT(1-u)^2\right]} \quad (1)$$

where N is Avogadro's constant, β is Bohr's magneton, k is Boltzmann's constant, and u is the well-known Langevin function [see Equation (2)].

 © 2010 Wiley-VCH Verlag GmbH & Co. KGaA, Weinheim

$$u = L\left(\frac{JS(S+1)}{kT}\right) = \coth\left(\frac{JS(S+1)}{kT}\right) - \frac{kT}{JS(S+1)} \quad (2)$$

The least-squares fitting of the magnetic susceptibility data led to $J = -0.02\ cm^{-1}$ and $g = 1.99$. The J value confirms the weak antiferromagnetic coupling between the Mn^{II} ions, which is consistent with the crystal structure of **1**, because the long ligands result in large distances between the Mn centers.

Compound **2** can be considered magnetically as a 1D compound, as from a magnetic point of view, the long azopy ligand cannot favor any noticeable magnetic coupling. Rueff et al.[42,43] proposed a phenomenological approach for some low-dimensional Co^{II} systems, which allows estimation of the strength of the antiferromagnetic exchange interactions. They postulate the phenomenological Equation (3).

$$\chi_M T = A[\exp(-E_1/kT)] + B[\exp(-E_2/kT)] \quad (3)$$

where $A + B$ are the Curie constant ($C \approx 2.8$–$3.4\ cm^3\,K\,mol^{-1}$ for octahedral Co^{II} ions) and E_1 and E_2 represent the "activation energies" corresponding to the spin–orbit coupling and the antiferromagnetic exchange interaction. Many good results have been reported in 1D Co^{II} compounds.[24,42–44] Moreover, it is in basic agreement with the experimental data obtained for compound **2** when using this model over the temperature range 6–300 K (Figure 10). The fit values obtained with this procedure are: $A + B = 3.65\ cm^3\,K\,mol^{-1}$, which basically agrees with those given in the literature for the Curie constant. $E_1/k = 49.33$ K is of the same magnitude as the values reported for 1D and 2D Co^{II} compounds. The value found for the antiferromagnetic exchange interaction, $E_2/k = 0.01$ K, is very weak, corresponding to $J = -0.02$ K for **2**. The small J value is compatible with the two long bridging ligands. The Curie–Weiss fit in the temperature range 27–300 K gave Curie constant $C = 3.58\ cm^3\,K\,mol^{-1}$ and Weiss constant $\theta = -16.71$ K, further indicating the antiferromagnetic interactions of **2** (Figure S3, Supporting Information).

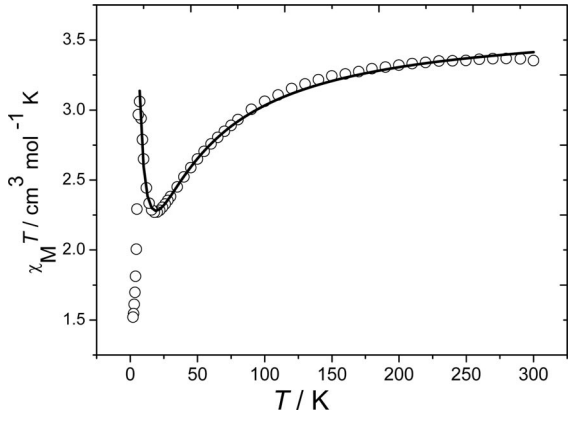

Figure 10. Plot of $\chi_M T$ (circle) of **2** and the corresponding fit according to the equation.

The Redox Properties of Complexes 1–3

For azo-type compounds, one of their unique characteristics is their redox properties.[39] The cyclic voltammograms of azopy in the solid-state were recorded. As shown in Figure 11a, free azopy diluted in carbon paste exhibits a couple of peaks ($E_{p,c} = -0.48$ V, $E_{p,a} = 0.18$ V vs. SCE, $\Delta E = 0.66$ V), which is similar to its chemical behavior in solution (DMF or acetonitrile).[45,46] This one-step reduction process may be based on the following reaction that is observed for azopy in aqueous buffer solution.[47]

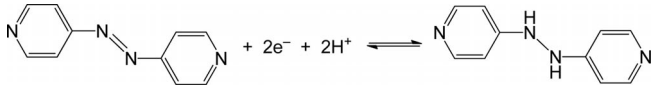

The electrochemical behaviors of compounds **1**, **2**, and **3** were characterized by cyclic voltammetry under the same conditions as those used in the solid state. As shown in Figure 11b, the electrochemical behavior of **1** shows only one pair of anodic and cathodic peaks. Furthermore, there are two differences between the two curves in Figure 11a,b. Firstly, the current density of the free azopy ligand is higher than that of **1**, indicating that the azopy ligand has less electrochemical activity after coordination with Mn^{II}. Secondly, the potential distinctness between the oxidation peak and the reduction peak is smaller than that for the free azopy ligand ($E_{p,c} = -0.16$ V, $E_{p,a} = 0.28$ V vs. SCE, $\Delta E = 0.44$ V). The reversibility of the electrochemical reaction in compound **1** is better than that of the free azopy ligand, and the reversible redox wave was still observed after four cycles (Figure S4, Supporting Information).

Figure 11c shows the CV curves of **2** in the solid state. Similarly to the free ligand, a couple of reduction and oxidation peaks appear ($E_{p,c} = -0.68$ V, $E_{p,a} = 0.43$ V vs. SCE, $\Delta E = 1.11$ V). This indicates that the potential distinctness between the oxidation peak and the reduction peak is larger than that of the free azopy ligand, whereas the current density of **2** is lower than that of the free ligands.

In contrast to the cases of **1** and **2**, **3** showed no obvious redox waves between –1.0 and 1.0 V, which is indicative of no apparent redox activity of the coordination-type azopy ligands. Thus, it is believed that the reversible redox waves observed for **1** and **2** are mainly attributed to the free azopy ligands, and there is no activity for the bridging azopy ligand.

Conclusions

In this paper, coordination compounds **1**–**3** were hydrothermally synthesized and structurally characterized. Compounds **1** and **2** are isostructural, and both exhibit 2D grid structures. Compound **3** possess an interesting 3D metal–organic framework with an unprecedented dodecadentate coordination mode and a unique $\{4^{16}.5^{10}.6^{18}.7\}\{4^4.5.6\}^2$ topology. This ideal net has not been encountered in MOF chemistry, and the topology has been deposited in the RSCR under the name zim. In addition, the cyclic voltammograms of **1**–**3** in the solid state showed that **1** and **2** have

 © 2010 Wiley-VCH Verlag GmbH & Co. KGaA, Weinheim

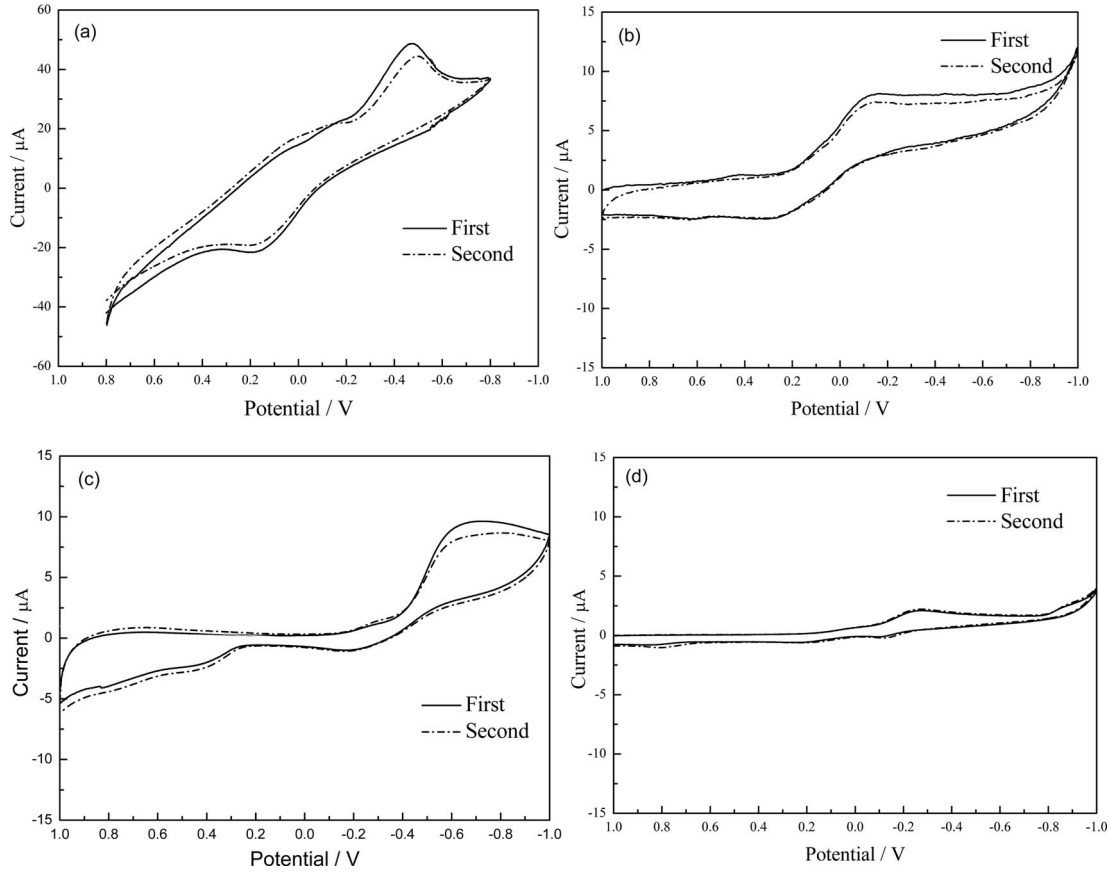

Figure 11. Cyclic voltammograms of (a) the free azopy ligand, (b) compound **1**, (c) compound **2**, and (d) compound **3**.

redox properties that are induced by the free azopy ligands, and **3** has no apparent redox activity. Moreover, magnetic studies revealed antiferromagnetic interactions between the metal ions in both **1** and **2**.

Experimental Section

General Materials and Methods: All chemicals were purchased from commercial sources and used without further purification. The azopy ligand was prepared according to a literature method.[48,49] Elemental analyses (C, H, and N) were performed with a Perkin–Elmer 240 CHN elemental analyzer. Powder X-ray diffraction (PXRD) measurements were recorded with a D/Max-2500 X-ray diffractometer by using Cu-K_α radiation. Variable-temperature magnetic susceptibilities were performed with a Quantum Design MPMS-7 SQUID magnetometer in the temperature range 2–300 K at 1000 Oe. Samples for magnetic measurements were ground into power to avoid anisotropy effects. Diamagnetic corrections were made with Pascal's constants for all the constituent atoms. Cyclic voltammograms were recorded with a BAS CV-50W polarographic analyzer. Each bulk sample of compounds **1**, **2**, and **3** was added to carbon paste (graphite and mineral oil) and mixed well, then the homogenized mixture was used to pack 3 mm inter diameter glass tubes. The surface was wiped with weighing paper, and electrical contact was established with a copper wire though the back of the electrode, which was used as a lead. Then, the working electrode was prepared. A SCE electrode was used as a reference, and a platinum wire was used as the counterelectrode. The three-electrode system was employed in 0.1 mol dm^{-3} $NaClO_4$ aqueous solution by using a scan rate of 10 mV s^{-1} in the range from –1.0 to 1.0 V.

{[Mn(H_2btec)(azopy)(H_2O)$_2$]·(azopy)}$_n$ (1): A mixture of $MnSO_4$·6H_2O (0.1369 g, 0.53 mmol), H_4btec (0.0254 g, 0.1 mmol), azopy (0.0184 g, 0.1 mmol), LiOH (0.0167 g, 0.4 mmol), and H_2O (10 mL) was stirred and then sealed in a 25-mL acid digestion Teflon-lined autoclave, which was heated at 140 °C for 3 d. After slow cooling to room temperature over an additional 3 d, salmon pink crystals (59% yield based on Mn) were collected after washing with water (2 × 5 mL) and drying in air. $C_{30}H_{24}MnN_8O_{10}$ (711.51): calcd. C 50.64, H 3.39, N 15.74; found C 50.26, H 2.95, N 15.39.

{[Co(H_2btec)(azopy)(H_2O)$_2$]·(azopy)}$_n$ (2): Compound **2** was prepared by a procedure similar to that for **1**, but with $CoSO_4$·6H_2O instead of $MnSO_4$·6H_2O. Red crystals (52% yield based on Co) were collected after washing with water (2 × 5 mL) and drying in air. $C_{30}H_{24}CoN_8O_{10}$ (715.45): calcd. C 50.35, H 3.38, N 15.66; found C 49.91, H 3.03, N 15.31.

{[$Zn_{2.5}$(btec)(azopy)(μ_3-OH)(H_2O)]·H_2O}$_n$ (3): Compound **3** was prepared by a procedure similar to that for **1**, but with $ZnSO_4$·6H_2O instead of $MnSO_4$·6H_2O. Salmon pink crystals (38% yield based on Zn) were collected after washing with water (2 × 5 mL) and drying in air. $C_{15}H_{11}N_2O_{11}Zn_{2.5}$ (558.77): calcd. C 32.24, H 1.98, N 5.01; found C 32.62, H 2.02, N 5.31.

X-ray Crystallography: Crystallographic data for **1**–**3** were collected with a Rigaku Saturn 007 CCD diffractometer, which was equipped with graphite monochromated Mo-K_α radiation (λ = 0.71073 Å). Structures were solved by direct methods with the SHELXS-97 program and refined by full-matrix least-squares tech-

 © 2010 Wiley-VCH Verlag GmbH & Co. KGaA, Weinheim

Table 2. Crystal data and structure refinement data of compounds **1**, **2** and **3**.

	1	**2**	**3**
Empirical formula	$C_{30}H_{24}MnN_8O_{10}$	$C_{30}H_{24}CoN_8O_{10}$	$C_{15}H_{11}N_2O_{11}Zn_{2.5}$
Formula mass	711.51	715.45	558.77
Crystal system	triclinic	triclinic	triclinic
Space group	$P\bar{1}$	$P\bar{1}$	$P\bar{1}$
Z	1	1	2
a / Å	9.0362(7)	8.996(2)	7.2951(19)
b /Å	9.6424(6)	9.671(2)	11.286(3)
c / Å	10.5281(6)	10.392(2)	11.694(3)
α / °	96.302(5)	96.873(17)	98.406(5)
β / °	114.865(7)	114.33(2)	102.479(5)
γ / °	105.231(6)	105.97(2)	106.219(5)
V / Å^3	777.22(9)	763.5(3)	880.5(4)
F(000)	365	361	550
$D_{calcd.}$ / g cm^{-3}	1.520	1.543	2.096
μ / mm^{-1}	0.497	0.635	3.458
Radiation (Mo-K_α) / Å	0.71073	0.71073	0.71073
T / K	293(2)	293(2)	293(2)
θ Range for data collection / °	2.53 to 25.01	2.55 to 26.44	3.66 to 25.00
Total reflections	5829	5131	4936
Independent reflections [$R_{(int)}$]	2745 [0.0290]	3057 [0.0393]	3033 [0.0411]
R_1, wR_2 [$I > 2\sigma(I)$]	0.0591, 0.1640	0.0715, 0.1930	0.0599, 0.1219
R_1, wR_2 (for all data)	0.0789, 0.1742	0.0939, 0.2071	0.0832, 0.1317
Goodness-of-fit on F^2	1.084	1.039	1.074
Maximum, minimum / e Å^{-3}	1.390, –0.589	2.616, –0.755	1.905, –0.849

niques against F^2 with the SHELXL-97 program package.[50] Lorentz polarization and adsorption corrections were applied by using the multiscan program. All non-hydrogen atoms in compounds **1**–**3** were refined anisotropically, and hydrogen atoms were located and refined isotropically. A summary of the crystallographic data for compounds **1**–**3** is provided in Table 2.

CCDC-756344 (for **1**), -756346 (for **2**), and -756349 (for **3**) contain the supplementary crystallographic data for this paper. These data can be obtained free of charge from The Cambridge Crystallographic Data Centre via www.ccdc.cam.ac.uk/data_request/cif.

Supporting Information (see also the footnote on the first page of this article): Powder XRD patterns of **1**–**3**, plots of $1/\chi$ vs. T for **1** and **2**, and the CV plot after four circles of **1**.

Acknowledgments

This work is supported by the National Natural Science Foundation of China (Grants 20631030 and 90922032) and the Ministry of Science and Technology of the People's Republic of China (MOST) (Grant 2007CB815305).

[1] M. O'Keeffe, M. A. Peskov, S. J. Ramsden, O. M. Yaghi, *Acc. Chem. Res.* **2008**, *41*, 1782–1789.
[2] Z. Wang, S. M. Cohen, *Chem. Soc. Rev.* **2009**, *38*, 1315–1329.
[3] O. M. Yaghi, M. O'Keeffe, N. W. Ockwing, H. K. Chae, M. Eddaoudi, J. Kim, *Nature* **2003**, *423*, 705–714.
[4] W. B. Yang, X. Lin, J. H. Jia, A. J. Blake, C. Wison, P. Hubberstey, N. R. Champness, M. Schröder, *Chem. Commun.* **2008**, 359–361.
[5] Y. G. Lee, H. R. Moon, Y. E. Cheon, M. P. Suh, *Angew. Chem. Int. Ed.* **2008**, *47*, 7741–7745.
[6] Y. L. Liu, J. F. Eubank, A. J. Cairns, J. Eckert, V. Ch. Kravtsow, R. Luebke, M. Eddaoudi, *Angew. Chem. Int. Ed.* **2007**, *46*, 3278–3283.
[7] G. J. McManus, Z. Q. Wang, D. A. Beauchamp, M. J. Zaworotko, *Chem. Commun.* **2007**, 5212–5213.
[8] J. J. Perry IV, J. A. Perman, M. J. Zaworotko, *Chem. Soc. Rev.* **2009**, *38*, 1400–1417.
[9] Y. C. Qiu, H. Deng, S. Yang, J. Mou, C. Daiguebonne, N. Kerbellec, O. Guillou, S. R. Batten, *Inorg. Chem.* **2009**, *48*, 3976–3981.
[10] B. K. Li, D. H. Olson, J. Y. Lee, W. Bi, T. Yuen, Q. Xu, J. Li, *Adv. Funct. Mater.* **2008**, *18*, 2205–2214.
[11] P. Cheng, S. P. Yan, C. Z. Xie, B. Zhao, X. Y. Chen, X. W. Liu, C. H. Li, D. Z. Liao, Z. H. Jiang, G. L. Wang, *Eur. J. Inorg. Chem.* **2004**, 2369–2378.
[12] H. Y. Liu, B. Zhao, W. Shi, Z. J. Zhang, P. Cheng, D. Z. Liao, S. P. Yan, *Eur. J. Inorg. Chem.* **2009**, 2599–2602.
[13] C. Janiank, *Dalton Trans.* **2003**, 2781–2804.
[14] S. Kitagawa, K. Uemura, *Chem. Soc. Rev.* **2005**, *34*, 109–119.
[15] W. Z. Shen, X. Y. Chen, P. Cheng, S. P. Yan, B. Zhai, D. Z. Liao, Z. H. Jiang, *Eur. J. Inorg. Chem.* **2005**, 2297–2305.
[16] X. Q. Zhao, Y. Zuo, D. L. Gao, B. Zhao, W. Shi, P. Cheng, *Cryst. Growth Des.* **2007**, *7*, 851.
[17] B. Zhao, P. Cheng, Y. Dai, C. Cheng, D. Z. Liao, S. P. Yan, Z. H. Jiang, G. L. Wang, *Angew. Chem. Int. Ed.* **2003**, *42*, 934–936.
[18] R. H. Wang, M. C. Hong, J. H. Luo, R. Cao, J. B. Weng, *Chem. Commun.* **2003**, *8*, 1018–1019.
[19] R. Vaidhyanathan, S. Natarajan, C. N. R. Rao, *Inorg. Chem.* **2002**, *41*, 4496–4501.
[20] A. C. Cerdeira, D. Sim, I. C. Santos, A. Machado, L. C. J. Pereira, *Inorg. Chim. Acta* **2008**, *361*, 3836–3840.
[21] T. Yamada, H. Kitagawa, *J. Am. Chem. Soc.* **2009**, *131*, 6312–6313.
[22] M. Fang, B. Zhao, Y. Zuo, J. Chen, W. Shi, J. Liang, P. Cheng, *Dalton Trans.* **2009**, 7765–7770.
[23] A. Mavrandonakis, E. Klontzas, E. Tylianakis, G. E. Froudakis, *J. Am. Chem. Soc.* **2009**, *131*, 13410–13414.
[24] S. C. Manna, E. Zangrando, J. Ribas, N. R. Chaudhuri, *Dalton Trans.* **2007**, 1383–1391.
[25] X. S. Wang, S. Ma, D. F. Sun, S. Parkin, H. C. Zhou, *J. Am. Chem. Soc.* **2006**, *128*, 16474–16475.
[26] H. T. Chung, H. L. Tsai, E. C. Yang, P. H. Chien, C. C. Peng, Y. C. Huang, Y. H. Liu, *Eur. J. Inorg. Chem.* **2009**, 3661–3666.

 © 2010 Wiley-VCH Verlag GmbH & Co. KGaA, Weinheim

[27] O. Shekhah, H. Wang, D. Zacher, R. A. Fischer, C. Woll, *Angew. Chem. Int. Ed.* **2009**, *48*, 5038–5041.
[28] S. Ma, J. M. Simmons, D. F. Sun, D. Q. Yuan, H. C. Zhou, *Inorg. Chem.* **2009**, *48*, 5263–5268.
[29] S. Hong, M. Oh, M. Park, J. W. Yoon, J. S. Chang, M. S. Lah, *Chem. Commun.* **2009**, 5397–5399.
[30] R. Prajapati, L. Mishra, K. Kimura, P. Raghavaiah, *Polyhedron* **2009**, *28*, 600–608.
[31] J. G. Vitillo, L. Regli, S. Chavan, G. Ricchiardi, G. Spoto, P. D. C. Dietzel, S. Bordiga, A. Zecchina, *J. Am. Chem. Soc.* **2008**, *130*, 8386–8396.
[32] Y. B. Wang, W. J. Zhuang, L. P. Jin, S. Z. Lu, *J. Mol. Struct.* **2005**, *737*, 165–172.
[33] D. Cheng, M. A. Khan, R. P. Houser, *Cryst. Growth Des.* **2002**, *2*, 415–420.
[34] M. T. Ding, J. Y. Wu, Y. H. Liu, K. L. Lu, *Inorg. Chem.* **2009**, *48*, 7457–7465.
[35] S. R. Caskey, A. J. Matzger, *Inorg. Chem.* **2008**, *47*, 7942–7944.
[36] a) D. Cheng, M. A. Khan, R. P. Houser, *Inorg. Chim. Acta* **2003**, *351*, 242–250; b) D. R. Xiao, E. B. Wang, H. Y. An, Y. G. Li, Z. M. Su, C. Y. Sun, *Chem. Eur. J.* **2006**, *12*, 2680–2691.
[37] L. N. Zhu, M. Liang, Q. L. Wang, W. Z. Wang, D. Z. Liao, Z. H. Jiang, S. P. Yan, P. Cheng, *J. Mol. Struct.* **2003**, *657*, 157–163.
[38] G. Agusti, S. Cobo, A. B. Gaspar, G. Molnár, N. O. Moussa, P. Á. Szilágyi, V. Pálfi, C. Vieu, M. C. Muñoz, J. A. Real, A. Bousseksou, *Chem. Mater.* **2008**, *20*, 6721–6732.
[39] S. Noro, M. Kondo, T. Ishii, S. Kitagawa, H. Matsuzaka, *J. Chem. Soc., Dalton Trans.* **1999**, 1569–1574.
[40] M. O'Keeffe, *Reticular Chemistry Structure Resource* (http://rcsr.anu.edu.au/).
[41] M. Menelaou, C. P. Raptopoulou, A. Terzis, V. Tangoulis, A. Salifoglou, *Eur. J. Inorg. Chem.* **2006**, 1957–1967.
[42] J. M. Rueff, N. Masciocchi, P. Rabu, A. Sironi, A. Skoulios, *Eur. J. Inorg. Chem.* **2001**, 2843–2848.
[43] J. M. Rueff, N. Masciocchi, P. Rabu, A. Sironi, A. Skoulios, *Chem. Eur. J.* **2002**, *8*, 1813–1820.
[44] F. P. Huang, H. Y. Li, J. L. Tian, W. Gu, Y. M. Jiang, S. P. Yan, D. Z. Liao, *Cryst. Growth Des.* **2009**, *9*, 3191–3196.
[45] J. L. Sadler, A. J. Bard, *J. Am. Chem. Soc.* **1968**, *90*, 1979–1989.
[46] A. J. Bellamy, I. S. MacKirdy, C. E. Niven, *J. Chem. Soc. Perkin Trans. 2* **1983**, 183–185.
[47] J. Haladjian, R. Pilard, P. Bianco, L. Asso, *Electrochim. Acta* **1985**, *30*, 695–699.
[48] P. J. Beadle, M. Goldstein, D. M. L. Goodgame, R. Grzeskowiak, *Inorg. Chem.* **1969**, *8*, 1490–1493.
[49] E. V. Brown, G. R. Granneman, *J. Am. Chem. Soc.* **1975**, *97*, 621–627.
[50] a) G. M. Sheldrick, *SHELXS 97: Program for the Solution of Crystal Structures*, University of Göttingen, Germany, **1997**; b) G. M. Sheldrick, *SHELXL 97: Program for the Refinement of Crystal Structures*, University of Göttingen, Germany, **1997**.

Received: December 28, 2009
Published Online: March 31, 2010

 © 2010 Wiley-VCH Verlag GmbH & Co. KGaA, Weinheim